JOURNAL OF BACTERIOLOGY, Apr. 2006, p. 2411–2420 Vol. 188, No. 7
0021-9193/06/$08.00+0 doi:10.1128/JB.188.7.2411–2420.2006

The First 45 Amino Acids of SopA Are Necessary for InvB Binding and SPI-1 Secretion

Wendy Higashide and Daoguo Zhou*

Department of Biological Sciences, Purdue University, West Lafayette, Indiana 47907

Received 21 October 2005/Accepted 11 January 2006

Salmonella enterica **serovar Typhimurium encodes two type III secretion systems (TTSSs) within pathogenicity island 1 (SPI-1) and island 2 (SPI-2). These type III protein secretion and translocation systems transport a panel of bacterial effector proteins across both the bacterial and the host cell membranes to promote bacterial entry and subsequent survival inside host cells. Effector proteins contain secretion and translocation signals that are often located at their N termini. We have developed a ruffling-based translocation reporter system that uses the secretion- and translocation-deficient catalytic domain of SopE, $SopE_{78–240}$, as a reporter. Using this assay, we determined that the N-terminal 45 amino acid residues of *Salmonella* SopA are necessary and sufficient for directing its secretion and translocation through the SPI-1 TTSS. $SopA_{1–45}$, but not $SopA_{1–44}$, is also able to bind to its chaperone, InvB, indicating that SPI-1 type III secretion and translocation of SopA require its chaperone.**

Salmonella spp. are the causes of many intestinal infections, ranging from mild gastroenteritis to severe typhoid fever. Once in the intestinal tract, *Salmonella* initiates infection by invading intestinal epithelial cells. The invasion ability is achieved through the type III protein secretion and translocation system encoded by *Salmonella* pathogenicity island 1 (SPI-1). Components of this type III protein transport system share extensive amino acid and architectural similarities with the flagellar export apparatus (19). The SPI-1 type III protein transport system functions to deliver a panel of bacterial virulence proteins, termed effectors, into the mammalian host cells. The secretion and subsequent translocation of SPI-1 type III effector proteins often require cognate chaperones (28).

It has been reported that signals that direct the secretion of these proteins are within the N-terminal amino acid or the mRNA sequences (1, 24, 25, 27, 30–32). The translocation signals that direct delivery of the proteins into host cells are thought to be located downstream near the secretion signal (37). Despite these advances in the characterization of these secretion signals, few studies have examined the effector translocation signals at a molecular level. A more complete analysis of these translocation signals may provide important clues as to how type III effector proteins traverse the host cell plasma membrane. This in turn may lead to the design of preventive and therapeutic pharmaceutical drugs that block the translocation of these virulence factors into mammalian cells. Toward this goal, we developed a ruffling-based translocation reporter system that uses the secretion- and translocation-deficient catalytic domain of SopE, $SopE_{78–240}$, as a reporter. Using this assay, we have done an extensive analysis of SopA, one of the SPI-1 type III secreted proteins translocated into host cells (38). Although this effector has been shown to have a role in inducing enteritis (38, 39), neither its biochemical activity in mammalian cells nor its secretion and translocation domains are known.

* Corresponding author. Mailing address: Department of Biological Sciences, Purdue University, West Lafayette, IN 47907. Phone: (765) 494-8159. Fax: (765) 494-0876. E-mail: zhoud@purdue.edu.

We report that the N-terminal 45 amino acid residues of *Salmonella* SopA are necessary and sufficient for its secretion and translocation into host cells. Interestingly, we found that full-length SopA is constitutively secreted through the flagellar export apparatus. In addition, secretion of SopA through the SPI-1 type III system required its chaperone, InvB, and its chaperone-binding domain.

MATERIALS AND METHODS

Bacterial strains and mammalian cell lines. Wild-type *Salmonella enterica* serovar Typhimurium strain SL1344 (SB300) and its *sopB* (SB933) null mutant derivative have been previously described (14, 42). The *sopB sopE* deletion mutant strain (ZP15) was constructed by introducing in-frame deletions of *sopE* and *sopB* into SB933 as described below. A DNA fragment containing the deletion (retaining the first two and last amino acids of *sopE*) was cloned into the R6K-derived suicide vector pSB890 (15) and introduced into the chromosome of SB933 by double homologous recombination. The resulting strain, ZP16, contains a SopE in-frame deletion in addition to the SopB C462S point mutation. The *sopB* deletion was then constructed in a similar manner by introducing an in-frame deletion of *sopB* (retaining the first and last amino acids) into ZP16, resulting in ZP15. The *flgGHI* deletion mutant (ZP88), the *invA flgGHI* deletion mutant (ZP89), the *sipC sopB sopE* deletion mutant (ZP91), and the *invB* deletion mutants (ZP143, ZP144, ZP145, and ZP146) were created similarly. *Salmonella* infection of mammalian cells was conducted as previously described (42). The human Henle-407 cell line (CCL-6), from the ATCC Cell Biology Stock Center (Manassas, VA), was maintained in Dulbecco's modified Eagle's medium supplemented with 10% bovine calf serum.

The SopA-M45 merodiploids were created by introducing the R6K-derived suicide vector pSB890 (16) carrying the 630-bp upstream sequence of *sopA*, followed by the sequence encoding SopA with an M45 epitope tag, into the chromosomes of the *Salmonella* strains. The upstream sequence of *sopA* and the sequence encoding SopA were amplified by PCR with the primers 5′-CTAGC TAGCGAACGACGACTAATGCTCATATAACC-3′ and 5′-TCCCCCGGGC GCCCAGGCCAG-3′ and then cloned into NheI and SmaI sites of pZP1139, replacing the $SopE_{78–240}$ reporter. The 3.048-kb NheI-BamHI fragment was then subcloned into the BamHI-XbaI sites of pSB890, resulting in pZP1251. Plasmid pZP1251 was then introduced into the chromosomes of SL1344, ZP143, SB136, ZP88, and ZP89, resulting in ZP152, ZP153, ZP154, ZP155, and ZP156, respectively.

Plasmid construction. The translocation reporter plasmid, pZP1139, was constructed to contain a multiple cloning site, the catalytic domain of SopE, and a C-terminal M45 epitope tag. The multiple cloning site and M45 epitope tag were created by cloning the annealed oligonucleotides 5′-AATTCCCATGGAGCTCAG ATCTGGTACCCCCGGGGGTGGTGCCATGGATCGGAGTAGGGATCGCC

TACCTCCTTTTGAGACAGAGACGCGGATCCTCT-3′ and 5′-CTAGAGGAT CCGCGTCTCTGTCTCAAAAGGAGGTAGGCGATCCCTACTCCGATCCAT ACCACCCCCGGGGGTACCAGATCTGAGCTCCATGGG-3′ into the EcoRI-XbaI sites of the pBAD derivative pSB1136 (13). The catalytic domain of $SopE_{78–240}$ was cloned upstream of the M45 epitope tag using the KpnI-SmaI-digested PCR fragments and primers 5′-GGGGTACCGGTGGTTTGACAAATAAAGTCGTT AAAG-3′ and 5′-CTTCTCTCATCCGCCAAAA-3′.

To generate $SopE_{78–240}$-M45 hybrid proteins fused to putative translocation signals, the genes encoding the corresponding proteins were amplified by PCR and cloned into pZP1139. The gene encoding SptP was amplified with primers 5′-GGAATTCTAATGCTAAAGTATGAGGAGAG-3′ and 5′-GGGGTAC CGCTTGCCGTCGTCATAAGCAACTG-3′ and then cloned into the EcoRI-KpnI sites of pZP1139, resulting in $SptP\text{-}SopE_{78–240}$-M45 (pZP0600). The *sptP* gene encoding $SptP_{1–101}$ (pZP0073) was amplified by PCR using primers 5′-G GAATTCTAATGCTAAAGTATGAGGAGAG-3′ and 5′-CCCAAGCTTAAC AGTGCGTCATTAAC-3′; the *sptP* gene encoding $SptP_{1–159}$ (pZP0071) was amplified with primers 5′-GGAATTCTAATGCTAAAGTATGAGGAGAG-3′ and 5′-GGGAAGCTTTTTTCTGCCACTTTTGT-3′. The PCR products were cloned into the EcoRI-SalI sites of pZP1139. The full-length *sopA* (pZP0800) was cloned into pZP1139 by ligating the BglII-EcoRI fragment of the PCR product using primers 5′-CCATCGATCGAAGGAATTCTAATGAAGATA-3′ and 5′-GAAGATCTCTCTAGACCACGCCCAGGCCAGT-3′. Genes encoding $SopA_{1–95}$ and $SopA_{1–45}$ were created by cloning the EcoRI-BamHI fragments of PCR products created from primers 5′-TGTTGATAAGGAATTCTA ATGAAGATA-3′ plus 5′-CGGGATCCGTTGCCTGCATTATTTGTATCTTT A-3′ and 5′-CGGGATCCGAAAGATGTATGCGTGTTTTTA-3′, resulting in pZP0776 and pZP0777, respectively. Genes encoding $SopA_{1–44}$ and $SopA_{1–35}$ were created by cloning the BssHII-SpeI fragments of PCR products using primers 5′-TTGGCGCGCGGACGAAAGTAAAC-3′ plus 5′-GACTAGTTGT ATGCGTGTTTTTAACACT G-3′ and 5′-GACTAGTTTTTGAGGTGAGCCC GTTTTTC-3′, resulting in pZP0866 and pZP0798, respectively. The $SopA_{1–45}$-Npt-M45 fusion construct (pZP1078) was created by cloning the BglII fragment of the PCR product using primers 5′-GAAGATCTATGAGCCATATTCAACGGGA AAC-3′ and 5′-GAGGATATCGAAAAACTCATCGAGCATCAAATGAA-3′ into the BglII-SmaI sites of pZP0777. Junctions of the final fusion plasmids were confirmed by DNA sequencing.

To modify the vector for the cyclic amp (cAMP) assay, the *Bordetella pertussis* adenylate cyclase gene was amplified by PCR using primers 5′-TCCCCCGGG CAGCAATCGCATCAGGCTGGTTA-3′ and 5′-AACTGCAGTCATCGATA ACTGTCATAGCCGGAATC-3′. The resulting 1.2-kb fragment was cloned into the PstI-SmaI sites of pZP1139 to produce pZP0599. The EcoRI-KpnI fragments of pZP776, pZP777, pZP800, and pZP866 were cloned into the same sites of pZP0599 to produce $SopA_{Full}$-CyaA (pZP0796), $SopA_{1–95}$-CyaA (pZP1084), $SopA_{1–45}$-CyaA (pZP1085), and $SopA_{1–44}$-CyaA (pZP1086), respectively. The EcoRI-SmaI fragments of pZP0071 and pZP0073 were cloned into the same sites of pZP0599 to produce $SptP_{1–159}$-CyaA (pZP0598) and $SopA_{1–101}$-CyaA (pZP0597), respectively.

Yeast two-hybrid constructs were created using pGADGH and pGBT9c vectors from CLONTECH (Palo Alto, CA). The gene encoding InvB was amplified with primers 5′-ACGCGTCGACATGCAACATTTGGATATCGCTGAATTA G-3′ and 5′-CCCAAGCTTTCATCTCATTAGCGACCGACTAAAAAC-3′, cloned into the HindIII-SmaI sites of pBlueScript SK, and then subcloned into pGADGH by the EcoRV-HindIII sites, resulting in pZP0901. The gene encoding SopA was PCR amplified with primers 5′-CGGGATCCATGAAGATAT CATCAGGCG-3′ and 5′-GGAATTCGCCTTAACTCCATGCGG-3′ and cloned into the BamHI-EcoRI sites in pGBT9c, resulting in pZP0061. DNA fragments encoding GAL4BD-$SopA_{1–45}$-Npt-M45 and GAL4BD-$SopA_{1–44}$-Npt-M45 were created by first replacing the $SopE_{78–240}$ tag with neomycin phosphotransferase (Npt) and by cloning the BglII-digested Npt PCR fragments using primers 5′-GAAGATCTATGAGCCATATTCAACGGGAAAC-3′ and 5′-GA GGATATCGAAAAACTCATCGAGCATCAAATGAA-3′ into the BglII-SmaI sites of pZP0777 and pZP0866, respectively. The DNA fragments encoding the fusion proteins were then cloned into the EcoRI and SmaI sites of pGBT9m, resulting in pZP1080 and pZP1064, respectively. GAL4BD-$SopA_{1–95}$-$SopE_{78–240}$-M45 (pZP1063) was created by cloning the 915-bp EcoRI-SalI fragment of pZP0776 into the same sites of pGBT9c.

Immunofluorescence microscopy. Henle-407 cells were infected for 30 min with *Salmonella* at a multiplicity of infection of 10 as described above. Infected cells were washed three times with phosphate-buffered saline (PBS) and fixed with 3% formaldehyde for 15 min at room temperature before permeabilization with 0.2% Triton X-100 in PBS. The cells were incubated with the primary antibody for 30 min after being blocked with 3% skim milk, washed three times with PBS, and incubated with the secondary antibody for 30 min. *S. enterica* serovar Typhimurium was identified using rabbit anti-*Salmonella* O antigen group B (Difco) and a secondary anti-rabbit AF488 conjugant (Molecular Probes, Eugene, OR). Actin was visualized by staining with Texas Red-conjugated phalloidin. The images represent black-and-white projections of z-section slices obtained on a Zeiss AxioVert 200 M deconvolution microscope. Pseudocolors were added by Adobe Photoshop.

Protein secretion and Western blotting. The *Salmonella* strains were grown under SPI-1-inducing conditions as described previously (9). To determine the secretion levels of the proteins, ZP15 expressing the fusion proteins (Table 1) was grown at 37°C for 12 h in LB-0.3 M NaCl medium. Bacterial cultures were diluted 1:100 in fresh LB-0.3 M NaCl medium. Cultures were grown with slow agitation for three additional hours. The production of fusion proteins from the pBAD promoter was induced by the addition of 0.05 mM arabinose during the last 2 h of growth. The bacteria were then pelleted by centrifugation at 10,000 × *g* for 20 min. The culture supernatants were passed through 0.2-μm filters, and the secreted proteins were collected by precipitation with 10% trichloroacetic acid. Cell lysates corresponding to 50 μl of bacterial culture and secreted proteins corresponding to 1.5 ml of culture supernatants were resuspended in sodium dodecyl sulfate-polyacrylamide gel electrophoresis (SDS-PAGE) sample buffer and separated by SDS-PAGE for Western blot analysis using anti-M45 (29) or anti-SipA (17) antibodies. Bacterial lysis was monitored using monoclonal anti-Hsp60 (3) antibodies, which were supplied by EMD Biosciences (Madison, WI).

Adenylate cyclase translocation assay. Bacterial cultures were grown and subcultured as described above. Henle-407 cells growing in 24-well tissue culture plates were infected with the above-mentioned subcultured *Salmonella* at a multiplicity of infection of 20. After 1 hour of infection, the cells were washed with ice-cold PBS buffer and then lysed with 0.1 M HCl with gentle agitation for 20 min. The lysate was tested for cAMP, using the Direct Immunoassay Kit (EMD Biosciences, Madison, WI) according to the manufacturer's instructions. Protein concentrations were determined using the Bio-Rad Protein Assay Kit (Hercules, CA) according to the manufacturer's instructions. Adenylate cyclase activity is expressed as pmol per microgram of total protein.

Far-Western blotting. Whole-cell lysates corresponding to 140 μl of *Escherichia coli* culture (optical density at 600 nm, 1.6) expressing SopA fusions were resolved by SDS-PAGE and transferred to nitrocellulose membranes. The membranes were blocked with 3% skim milk in 50 mM Tris (pH 7.5), 100 mM sodium acetate, 350 mM sodium chloride, 1 mM EDTA, 5 mM $MgCl_2$, and 0.3% Tween supplemented with 1 mM dithiothreitol for 3 h. The membranes were then probed with glutathione *S*-transferase (GST)-InvB or GST protein (2 μg/ml), followed by polyclonal anti-GST and Alexa Fluor 680-conjugated goat anti-rabbit antibodies (Molecular Probes, Eugene, OR). The blots were visualized and recorded with the Odyssey Infrared Imaging System (LI-COR Biosciences, Lincoln, NE).

Yeast two-hybrid assay. The GAL4-based yeast two-hybrid system was used following standard procedures (2). The bait plasmids were constructed by fusing DNA fragments encoding SopA, $SopA_{1–95}$-$SopE_{78–240}$-M45, $SopA_{1–45}$-Npt-M45, and $SopA_{1–44}$-Npt-M45 in frame to the yeast GAL4 binding domain in pGBT9. The prey, InvB, was fused to the GAL4 activation domain from pGADGH. The positive control plasmids, GAL4-BD-$SipA_{459–684}$ (pSB1025) and GAL4-AD-Plastin (pSB1014), were described previously (41). The yeast indicator strain, Y153, was cotransformed using a protocol described previously (2). The β-galactosidase assay was performed as previously described (34).

RESULTS

$SopA_{1–45}$, but not $SopA_{1–44}$, is translocated into host cells. In order to facilitate the identification of SPI-1 type III translocation signals, we developed a translocation reporter system that uses the secretion- and translocation-deficient catalytic domain of SopE (78 to 240 amino acids) as a reporter. This reporter system takes advantage of the fact that a *Salmonella* strain with null mutations in SopE and SopB is severely impaired in producing cytoskeletal rearrangements in the host cells (40). Transient expression of $SopE_{78–240}$, the catalytic domain lacking its chaperone-binding domain, is able to induce membrane ruffling in mammalian cells (12). If a complete translocation sequence is cloned upstream of the catalytic domain of SopE and introduced into the *sopB sopE* mutant strain

TABLE 1. Bacterial strains and plasmids

Strain or plasmid	Relevant characteristics	Source
S. enterica serovar Typhimurium		
SL1344	Wild-type *S. enterica* serovar Typhimurium; Str^r	14
SB136	SL1344 *invA*::*aphT*	10
SB933	SL1344 $sopB_{C462S}$	42
ZP15	SL1344 Δ*sopB* Δ*sopE*	This study
ZP16	SL1344 $sopB_{C462S}$ Δ*sopE*	This study
ZP88	SL1344 Δ*flgGHI*	This study
ZP89	SB136 Δ*flgGHI*	This study
ZP91	ZP15 Δ*sipC*	This study
ZP143	SL1344 Δ*invB*	This study
ZP144	SB136 Δ*invB*	This study
ZP145	ZP88 Δ*invB*	This study
ZP146	ZP89 Δ*invB*	This study
ZP152	SL1344 *sopA*::pZP1251	This study
ZP153	ZP143 *sopA*::pZP1251	This study
ZP154	SB136 *sopA*::pZP1251	This study
ZP155	ZP88 *sopA*::pZP1251	This study
ZP156	ZP89 *sopA*::pZP1251	This study
E. coli		
DH5Amcr	F^- *mcrA* Δ(*mrr-hsdRMS-mcrBC*)	Gibco BRL
SM10 λ*pir*	*thi thr leu tonA lacY supE recA*::RP4-2-Tc::Mu (Knr) λ*pir*	26
Saccharomyces cerevisiae		
Y153	URA3::GAL1-lacZLYS2:GAL1-HIS3	Clontech
Plasmids		
pSB890	R6K-derived *ori*; Tc^r	16
pSB1014	pGADGH derivative; GAL4AD-T-Plastin	41
pSB1025	pGBT9 derivative; GAL4BD-$SipA_{459–684}$	41
pSB1136	pBAD derivative; SopE-M45 fusion vector	12
pZP0061	pGBT9 derivative; GAL4BD-SopA	This study
pZP0071	pSB1136 derivative; $SptP_{1–159}$-$SopE_{78–240}$-M45	This study
pZP0073	pSB1136 derivative; $SptP_{1–101}$-$SopE_{78–240}$-M45	This study
pZP0597	pZP1139 derivative; $SptP_{1–101}$-CyaA	This study
pZP0598	pZP1139 derivative; $SptP_{1–159}$-CyaA	This study
pZP0599	pZP1139 derivative; CyaA	This study
pZP0600	pZP1139 derivative; SptP- $SopE_{78–240}$-M45	This study
pZP0776	pZP1139 derivative; $SopA_{1–95}$-$SopE_{78–240}$-M45	This study
pZP0777	pZP1139 derivative; $SopA_{1–45}$-$SopE_{78–240}$-M45	This study
pZP0796	pZP1139 derivative; SopA-CyaA	This study
pZP0798	pZP1139 derivative; $SopA_{1–35}$-$SopE_{78–240}$-M45	This study
pZP0800	pZP1139 derivative; SopA-$SopE_{78–240}$-M45	This study
pZP0866	pZP1139 derivative; $SopA_{1–44}$-$SopE_{78–240}$-M45	This study
pZP0901	pGADGH derivative; GAL4AD-InvB	This study
pZP1063	pGBT9 derivative; GAL4BD-$SopA_{1–95}$-$SopE_{78–240}$-M45	This study
pZP1064	pGBT9 derivative; GAL4BD-$SopA_{1–44}$-Npt-M45	This study
pZP1078	pZP1139 derivative; $SopA_{1–45}$-Npt-M45	This study
pZP1080	pGBT9 derivative; GAL4BD-$SopA_{1–45}$-Npt-M45	This study
pZP1084	pZP1139 derivative; $SopA_{1–95}$-CyaA	This study
pZP1085	pZP0599 derivative; $SopA_{1–45}$-CyaA	This study
pZP1086	pZP0599 derivative; $SopA_{1–44}$-CyaA	This study
pZP1139	pSB1136 derivative; $SopE_{78–240}$-M45	This study
pZP1251	pSB890 derivative; 630-bp upstream sequence of SopA; SopA-M45	This study

(ZP15), the expression and subsequent translocation of this chimeric protein into host cells will result in actin cytoskeletal rearrangements (Fig. 1). This assay is a very sensitive tool for detecting translocation, because cellular responses are observed before those detected by biochemical means (unpublished data). Previously, it has been reported that the first 159 amino acids, but not the first 101 amino acids, of SptP are sufficient for translocation (7, 37). As expected, actin cytoskeletal rearrangements were observed when Henle-407 cells were infected with ZP15 expressing $SptP_{1–159}$-$SopE_{78–240}$-M45. In contrast, ZP15 expressing $SptP_{1–101}$-$SopE_{78–240}$ did not induce noticeable ruffles (Fig. 1), nor did cells infected with ZP15 expressing $SopE_{78–240}$-M45 (data not shown). These results demonstrate that it is possible to use $SopE_{78–240}$ as a reporter for determining the minimal secretion and translocation region by the induction of cytoskeletal rearrangements.

To define the secretion and translocation signal(s) of SopA, we constructed several C-terminal deletions of SopA. Expres-

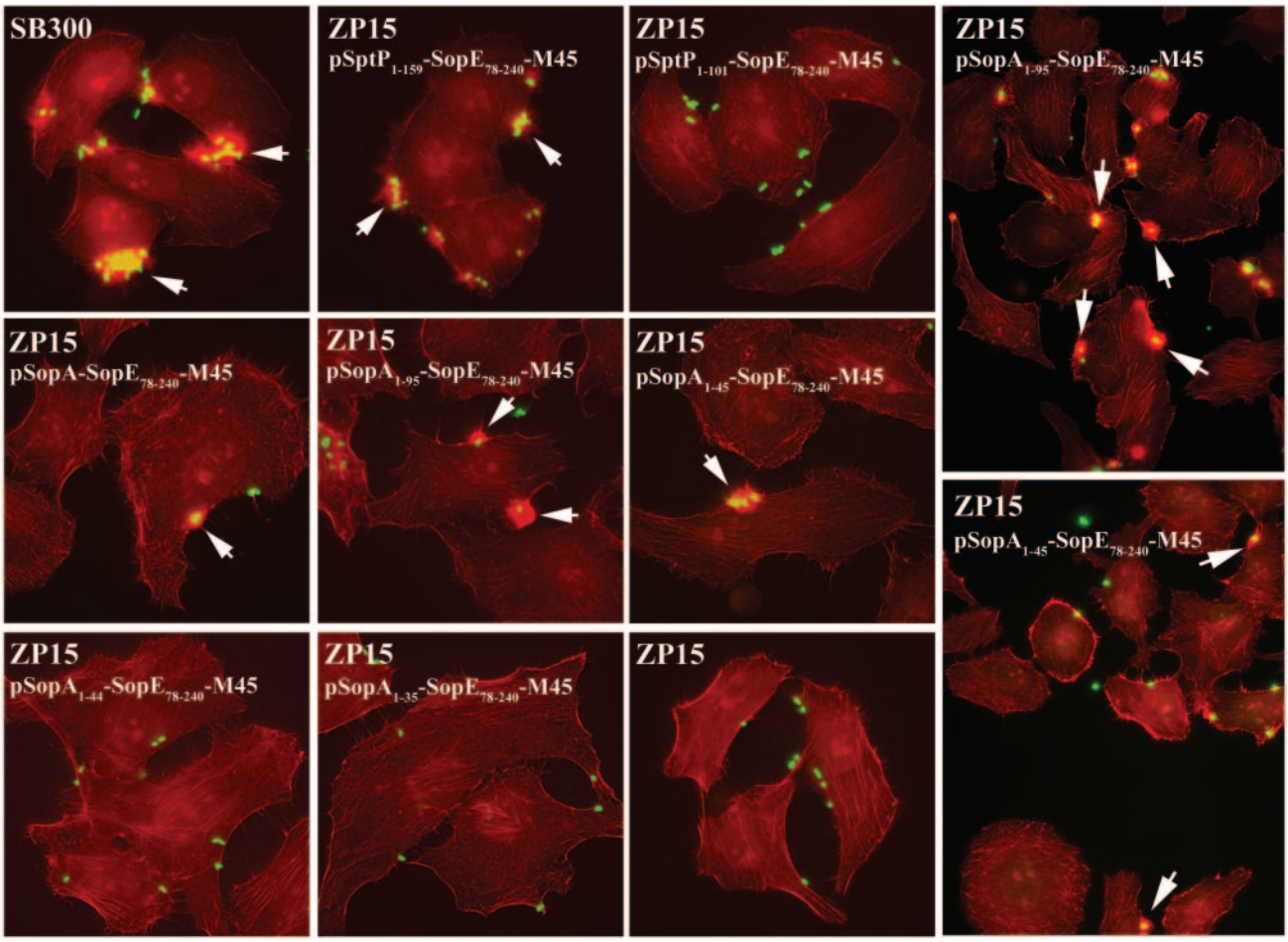

FIG. 1. Amino acids 1 to 45 of SopA were sufficient to translocate $SopE_{78–240}$-M45 and induce actin cytoskeletal rearrangements in Henle-407 cells. Henle-407 cells were infected for 30 min with a *sopB sopE* double mutant (ZP15) expressing $SopE_{78–240}$-M45 fusions. Infected cells were processed to visualize F actin (red) and *Salmonella* (green). The arrows indicate locations of membrane ruffles.

sion of the fusion proteins was under the control of an arabinose-inducible promoter of a pBAD24 derivative, pZP1139 (12). As shown in Fig. 1, the full-length SopA-$SopE_{78–240}$-M45 induced moderate membrane ruffles. Interestingly, infection with the ZP15 strain expressing the $SopA_{1–95}$-$SopE_{78–240}$-M45 fusion protein had very pronounced actin cytoskeletal rearrangements, which were more frequent and larger than those induced by the full-length SopA. We also found that ruffling was observed with the first 45 amino acids, but no ruffling was evident when cells were infected with ZP15 expressing $SopA_{1–35}$-$SopE_{78–240}$-M45 or $SopA_{1–10}$-$SopE_{78–240}$-M45 (Fig. 1 and data not shown). To precisely delineate the minimal secretion and translocation region, additional single-amino-acid deletions within this region were constructed, and their activities to induce actin cytoskeletal rearrangements were tested. As seen in Fig. 1, $SopA_{1–44}$-$SopE_{78–240}$-M45 failed to induce noticeable actin cytoskeletal rearrangements comparable to those induced by the negative control and $SopA_{1–35}$-$SopE_{78–240}$-M45. These data indicate that the minimal secretion and translocation signal of SopA lies within the N-terminal 45 amino acids.

To further demonstrate that the inability of $SopA_{1–44}$-$SopE_{78–240}$-M45 to induce actin cytoskeleton rearrangements is due to the lack of its translocation into mammalian cells, the translocations of SopA-$SopE_{78–240}$, $SopA_{1–95}$-$SopE_{78–240}$, $SopA_{1–45}$-$SopE_{78–240}$, and $SopA_{1–44}$-$SopE_{78–240}$ were further analyzed using the adenylate cyclase assay in Henle-407 cells (36). For this assay, the $SopE_{78–240}$-M45 tag of the SopA constructs was replaced with the *Bordetella pertussis cyaA* gene, and the translocation was measured by monitoring the concentration of cAMP. SopA-CyaA, $SopA_{1–95}$-CyaA, $SopA_{1–45}$-CyaA, and $SopA_{1–44}$-CyaA were expressed in ZP15 and ZP91, an isogenic ZP15 strain with an additional in-frame deletion in SipC, which is defective in translocation. $SptP_{1–159}$-CyaA and $SptP_{1–101}$-CyaA were used as positive and negative controls for translocation, respectively. As shown in Fig. 2, SopA-CyaA, $SopA_{1–95}$-CyaA, and $SopA_{1–45}$-CyaA were translocated in a SipC-dependent manner. However, the $SopA_{1–44}$-CyaA fusion protein yielded only background levels of adenylate cyclase activity similar to that induced by a *sipC* null mutant strain. The cAMP levels of $SopA_{1–44}$-CyaA were slightly, but significantly ($P < 0.06$; Student's *t* test), lower than the cAMP levels of $SopA_{1–45}$-CyaA

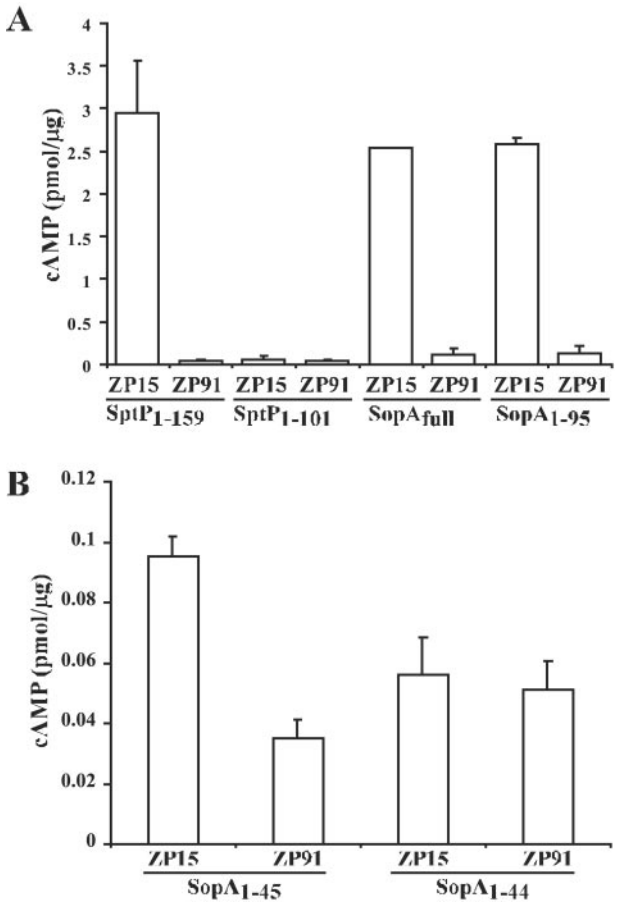

FIG. 2. Translocation of SopA-CyaA, $SopA_{1–95}$-CyaA, and $SopA_{1–45}$-CyaA into the Henle-407 cells. Intracellular cAMP levels are an indication of the translocation of CyaA fusion proteins in *Salmonella* ZP15 (*sopB sopE*) and ZP91 (*sipC sopB sopE*) strains. Cells were infected for 1 h, and the adenylate cyclase activity was determined. The data were from three independent experiments, with standard deviations shown as error bars. cAMP values are presented as pmol per microgram of total cellular protein.

that were averaged from three independent experiments. Together with the translocation ruffling assay, this confirms that the minimal region of SopA for secretion and translocation is within the first 45 amino acids.

$SopA_{1–45}$ is secreted through both the flagellar export apparatus and the SPI-1 type III secretion system (TTSS), while $SopA_{1–44}$ is secreted only by the flagellar export apparatus. The lack of translocation of $SopA_{1–44}$ could have resulted from a lack of either secretion or translocation or a deficiency in both processes. To determine the secretion abilities of these fusion constructs, culture supernatants from the wild-type *Salmonella* strain (SL1344), a flagellar-export-deficient mutant strain (*flgGHI*; ZP88), an SPI-1 type III secretion-deficient mutant strain (*invA*; SB136), and a mutant deficient in both secretion apparatuses (*flgGHI invA*; ZP89) carrying plasmids expressing $SopA_{full}$-$SopE_{78–240}$-M45, $SopA_{1–45}$-$SopE_{78–240}$-M45, or $SopA_{1–44}$-$SopE_{78–240}$-M45 were analyzed by Western blotting. As seen in Fig. 3, all the fusion proteins were secreted from the wild-type and *invA* mutant strains. In addition, $SopA_{full}$-$SopE_{78–240}$-M45 and $SopA_{1–45}$-$Sop_{78–240}$-M45 were also secreted from the *flgGHI* mutant strain (Fig. 3). However, the secretion of $SopA_{full}$-$SopE_{78–240}$-M45 and $SopA_{1–45}$-$Sop_{78–240}$-M45 was completely abolished in the *flgGHI invA* mutant strain, indicating that they are secreted by both the flagellar export apparatus and SPI-1 TTSS. In contrast, the secretion of $SopA_{1–44}$-$SopE_{78–240}$-M45 was detected only in the culture supernatants of the wild-type and the *invA* mutant strains but was absent from supernatants of both the *flgGHI* mutant and the *flgGHI invA* mutant strains (Fig. 3). Similar to $SopA_{1–44}$-$SopE_{78–240}$-M45, the secretion of $SopA_{1–10}$-$SopE_{78–240}$-M45 and $SopA_{1–35}$-$SopE_{78–240}$-M45 was detected only in the culture supernatants of the wild-type and the *invA* mutant strains but was absent from supernatants of both the *flgGHI* mutant and the *flgGHI invA* mutant strains (data not shown). The lack of detectable secretion in the *flgGHI* mutant strain indicates the inability of $SopA_{1–44}$-$SopE_{78–240}$-M45 to be secreted by the

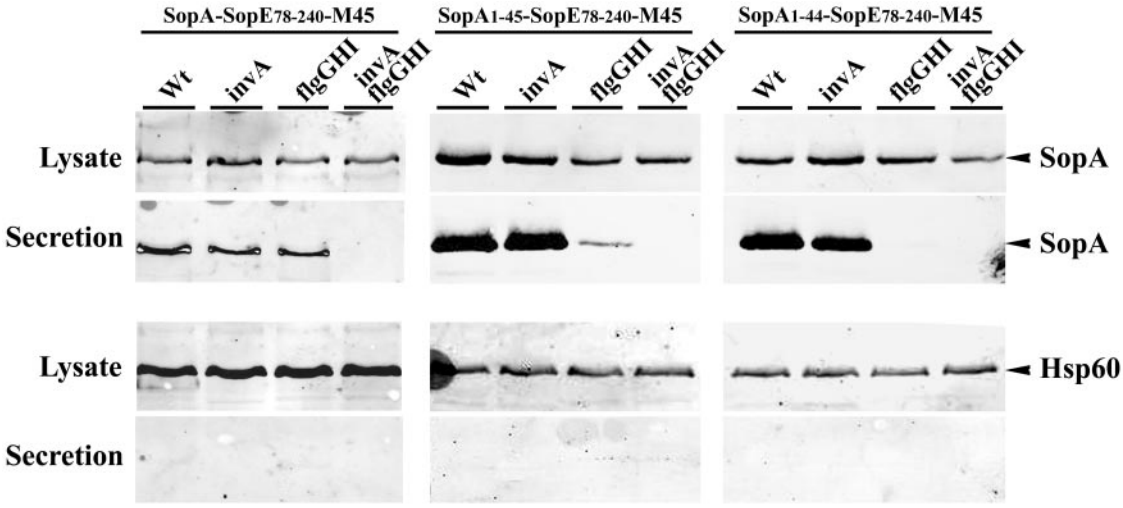

FIG. 3. Secretion profiles of $SopA_{full}$-$SopE_{78–240}$-M45, $SopA_{1–45}$-$SopE_{78–240}$-M45, and $SopA_{1–44}$-$SopE_{78–240}$-M45 fusion proteins. The cell lysate samples corresponded to 50 μl of culture, and the secreted proteins corresponded to 1.5 ml of culture supernatant. Full-length and C-terminal deletions of SopA were fused to $SopE_{78–240}$-M45 using the translocation reporter plasmid. Their expression and secretion were examined by Western blotting in the wild-type (Wt) strain (SL1344), an SPI-1 type III secretion-deficient mutant strain (*invA*; SB136), a flagellar-export-deficient mutant strain (*flgGHI*; ZP88), and a mutant deficient in both secretion apparatuses (*flgGHI invA*; ZP89). Leakage and bacterial lyses were monitored using monoclonal anti-Hsp60 antibodies.

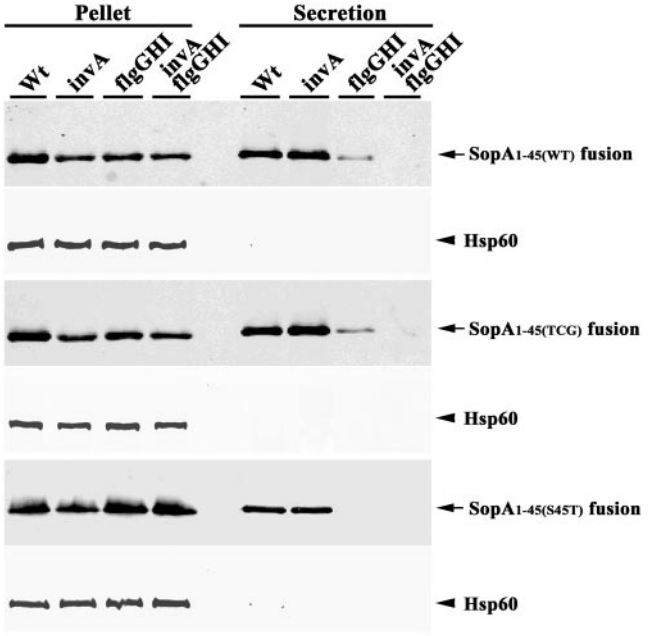

FIG. 4. Secretion profiles of $SopA_{1–45}$-$SopE_{78–240}$-M45, $SopA_{1–45}$ (the serine codon at position 45 from TCT to TCG)-$SopE_{78–240}$-M45, and $SopA_{1–45}$ (S45T)-$SopE_{78–240}$-M45 fusion proteins. The cell lysates corresponded to 50 μl of culture, and secreted proteins corresponded to 1.5 ml of culture supernatant. Their expression and secretion were examined by Western blotting in the wild-type (Wt) strain (SL1344), an SPI-1 type III secretion-deficient mutant strain (*invA*; SB136), a flagellar-export-deficient mutant strain (*flgGHI*; ZP88), and a mutant deficient in both secretion apparatuses (*flgGHI invA*; ZP89).

SPI-1 type III secretion system. As a control for bacterial lysis and/or nonspecific leakage, the presence of Hsp60, a cytosolic heat shock protein, was also determined in the same blot. No Hsp60 was detected in the supernatant from any of the strains used in this study (Fig. 3).

There have been many studies of *Yersinia* effectors to determine whether the type III secretion signal is found in the mRNA sequence or in the protein sequence (11, 23, 32). A similar investigation of *Salmonella* identified the N-terminal amino acid sequence as the secretion signal for SopE (18). To determine if the mRNA sequence, and not the amino acid sequence, was responsible for this difference in secretion between $SopA_{1–45}$-$SopE_{78–240}$-M45 and $SopA_{1–44}$-$SopE_{78–240}$-M45, the serine (S45) was mutated to the corresponding five silent mutations (codon TCT to TCC, TCA, TCG, AGT, and AGC) by site-directed mutagenesis. The secretion profiles of these constructs were found to be identical to that of the $SopA_{1–45}$-$SopE_{78–240}$-M45 construct in the wild-type and *invA*, *flgGHI*, and *flgGHI invA* mutant strains (Fig. 4 and data not shown). To further investigate the critical role of S45 in secretion, we also mutated the serine 45 to a threonine in $SopA_{1–45}$-Sop $E_{78–240}$-M45 and examined the secretion profile of the mutated $SopA_{1–45}$-$SopE_{78–240}$-M45 (S45T) in the above-mentioned four *Salmonella* strains. We found that $SopA_{1–45}$-$SopE_{78–240}$-M45 (S45T) was secreted in a manner identical to that of $SopA_{1–44}$-$SopE_{78–240}$-M45 (Fig. 4). This result indicates that the loss of serine 45, or a modification of it to a threonine, prevented secretion through the SPI-1 type III secretion apparatus. Taken together, our data demonstrate that serine 45 is critical for secretion and translocation through the SPI-1 type III secretion apparatus.

To determine if SPI-1 and/or flagellar secretion of $SopA_{full}$-$SopE_{78–240}$-M45, $SopA_{1–45}$-$SopE_{78–240}$-M45, and $SopA_{1–44}$-$SopE_{78–240}$-M45 is dependent on the SopA chaperone, InvB, we examined the secretion profiles of these constructs in *invB*, *invB invA*, *invB flgGHI*, and *invB invA flgGHI* strains. We found that the SPI-1 secretion of $SopA_{full}$-$SopE_{78–240}$-M45 and $SopA_{1–45}$-$SopE_{78–240}$-M45 that was observed from the *flgGHI* strain was InvB dependent (Fig. 3 and 5A). Secretion through the flagellar export apparatus of $SopA_{full}$-$SopE_{78–240}$-M45, $SopA_{1–45}$-$SopE_{78–240}$-M45, and $SopA_{1–44}$-$SopE_{78–240}$-M45 was not affected between the *invA* and the *invA invB* mutants (Fig. 5B). These data indicate that $SopA_{full}$-$SopE_{78–240}$-M45 and $SopA_{1–45}$-$SopE_{78–240}$-M45 secretion through SPI-1, but not through the flagellar export apparatus, requires its chaperone, InvB.

To eliminate the possibility that the secretion of the SopA fusion proteins by the *invA* mutant was due to overexpression of the fusion proteins from the pBAD derivative plasmid, SopA-M45 was introduced into the chromosome with a suicide plasmid in the wild-type, *invB* mutant, *invA* mutant, *flgGHI* mutant, and *flgGHI invA* mutant *Salmonella* strains. In these strains, SopA-M45 is expressed from its native promoter in the chromosome. As seen in Fig. 6, with the exception of the *invB* mutant, the merodiploid strains expressed SopA-M45 in approximately equivalent amounts. The lower SopA-M45 expression in the *invB* mutant strain is likely due to the fact that InvB is required for SopA expression (6). Similar to the secretion of the SopA fusion proteins expressed from the plasmid, the chromosomal SopA-M45 was secreted by the *invA* mutant, but not in the mutant that was deficient in both the flagellar export apparatus and SPI-1 TTSS. This phenomenon appears to be specific to SopA, because another SPI-1 TTS effector, SipA, was not secreted by the *invA* mutant (Fig. 6). Collectively, the data indicate that the deficiency in translocation of $SopA_{1–44}$ is likely due to its inability to be secreted through the SPI-1 TTS apparatus.

$SopA_{1–45}$, but not $SopA_{1–44}$, interacts with its chaperone, InvB. In addition to being the chaperone for SipA, SopE, and SopE2 (4, 21), InvB has been identified as the SopA chaperone (6). To further understand the molecular mechanisms that underlie the secretion and translocation of SopA, the interaction of $SopA_{1–45}$ and $SopA_{1–44}$ with InvB was examined by yeast two-hybrid and protein overlay analyses. The yeast two-hybrid assay employed fusions of the DNA-binding domain of GAL4 and SopA (GAL4BD-SopA) and the activation domain of GAL4 and InvB (GAL4AD-InvB). Because the C-terminal deletions of SopA were not expressed well alone, the $SopE_{78–240}$ reporter was retained in these constructs. To ensure that the interaction was not dependent on the $SopE_{78–240}$ tag, we also replaced the $SopE_{78–240}$ tag with Npt. Yeast strains carrying plasmids expressing GAL4BD-SopA, GAL4BD-$SopA_{1–95}$-$SopE_{78–240}$, and GAL4BD-$SopA_{1–45}$-Npt with plasmids expressing GAL4AD-InvB grew well on the yeast drop-out media lacking histidine (Fig. 7A). This interaction was not detected with yeast expressing GAL4BD-$SopA_{1–44}$-Npt and GAL4AD-InvB, nor when GAL4AD-Plastin was expressed in place of GAL4AD-InvB (Fig. 7A). In addition, yeast strains carrying GAL4BD-SopA, GAL4BD-$SopA_{1–95}$-$SopE_{78–240}$, and GAL4BD-$SopA_{1–45}$-Npt

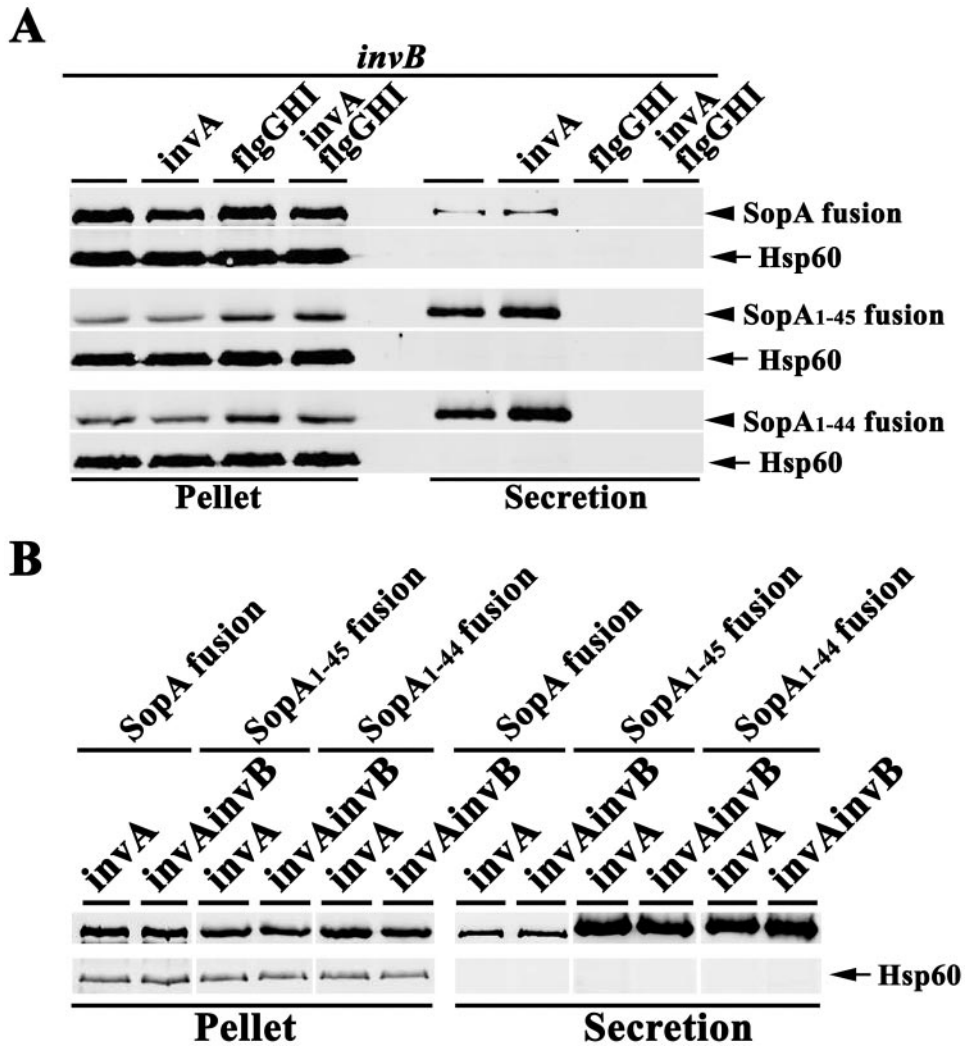

FIG. 5. Secretion profiles of $SopA_{full}$-$SopE_{78–240}$-M45, $SopA_{1–45}$-$SopE_{78–240}$-M45, and $SopA_{1–44}$-$SopE_{78–240}$-M45 fusion proteins in *invB* (A) and *invA* (B) mutant derivatives. The cell lysates corresponded to 50 μl of bacterial culture, and the secreted proteins corresponded to 1.5 ml of culture supernatant. The expression and secretion of $SopA_{full}$-$SopE_{78–240}$-M45, $SopA_{1–45}$-$SopE_{78–240}$-M45, and $SopA_{1–44}$-$SopE_{78–240}$-M45 were examined by Western blotting in *invA* (SB136), *invB* (ZP143), *invA invB* (ZP144), *invB flgGHI* (ZP145), and *invB flgGHI invA* (ZP146) strains. Leakage and bacterial lyses were monitored using monoclonal anti-Hsp60 antibodies.

together with GAL4AD-InvB exhibited β-galactosidase activity using a filter lift assay (Fig. 7A). No β-galactosidase activity was detected from yeast strains expressing GAL4BD-Sop $A_{1–44}$-Npt and GAL4AD-InvB, nor with the negative controls, GAL4BD-$SopA_{1–45}$-$SopE_{78–240}$ and GAL4AD-Plastin.

The interaction between $SopA_{1–45}$ and InvB was investigated further by a protein overlay assay. Whole-cell lysates of *E. coli* DH5α expressing $SopA_{1–95}$-$SopE_{78–240}$-M45, $SopA_{1–45}$-$SopE_{78–240}$-M45, $SopA_{1–45}$-Npt-M45, and $SopA_{1–44}$-$SopE_{78–240}$-M45 were separated by SDS-PAGE and immobilized onto nitrocellulose membranes. As a negative control, SptP, whose chaperone is SicP (7), was tested in a similar manner. Immobilized membranes were probed with either purified GST-InvB or GST alone, followed by anti-GST antibodies (Fig. 7B). The GST-InvB probe bound well to the $SopA_{1–95}$-$SopE_{78–240}$-M45 and $SopA_{1–45}$-$SopE_{78–240}$-M45 fusion constructs. This interaction was not observed for $SopA_{1–44}$-$SopE_{78–240}$-M45 or for SptP-$SopE_{78–240}$-M45, which does not interact with InvB. In addition, no interactions were observed when the blots were probed with GST instead of GST-InvB (data not shown). Interaction was also observed between GST-InvB and the $SopA_{1–45}$-Npt-M45 fusion proteins, indicating that the specificity between InvB and $SopA_{1–45}$-$SopE_{78–240}$ was independent of the $SopE_{78–240}$ fragment. Taken together, these experiments demonstrated that InvB interacts with $SopA_{1–45}$, but not with $SopA_{1–44}$.

DISCUSSION

Previous methods of defining the type III secretion and translocation domains included the digitonin subcellular fractionation technique (22), fluorescence staining (8, 33), the adenylate cyclase assay (36), and the phospho-Elk assay (5). They have been used effectively to characterize the type III effector translocation domains. We developed a ruffling-based translo-

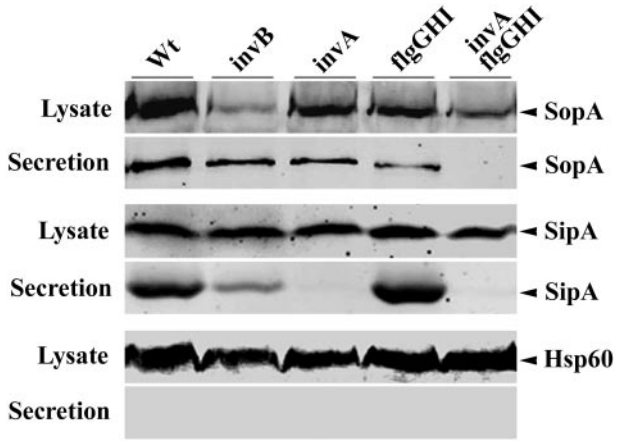

FIG. 6. Chromosomally expressed SopA-M45 is secreted by the *invA* mutant. Using a suicide vector, SopA-M45 was introduced into the chromosome of the wild-type (Wt) strain (SL1344), a mutant strain that contains an in-frame deletion in the gene that encodes the SopA chaperone (*invB*), an SPI-1 type III secretion-deficient mutant strain (*invA*; SB136), a flagellar-export-deficient mutant strain (*flgGHI*; ZP88), and a mutant deficient in both secretion apparatuses (*flgGHI invA*; ZP89). The secretion of SipA and SopA-M45 was examined by Western blotting with anti-SipA and anti-M45 antibodies. The lysate sample corresponded to 200 μl of bacterial culture, and the secretion sample corresponded to 6 ml of culture supernatant. The blot was reprobed with anti-Hsp60 to detect nonspecific leakage and bacterial lysis.

cation reporter system that uses the secretion- and translocation-deficient catalytic domain of SopE, $SopE_{78–240}$, as a reporter. By itself, $SopE_{78–240}$ is not translocated into mammalian cells, but it is capable of inducing actin cytoskeleton rearrangements once fused to proper secretion and translocation signals. Since SopE is itself secreted and translocated via the SPI-1 type III protein secretion system, the putative type III secretion and translocation signals fused to it have little adverse effect on its secretion and translocation. In addition, our assay is based on the ruffling phenotype induced by $SopE_{78–240}$. There are no false positives, because $SopE_{78–240}$ is translocation deficient. Our ruffling assay is more suitable for qualitative analysis to define the minimum region that is capable of translocation and, thus, of inducing ruffles. The dynamic nature of the ruffles (different shapes and sizes) often prevents accurate quantitative measurements. Although the *sopE sopB* double mutant is still able to translocate SipA, SipC, and SopE2, no obvious actin rearrangements were observed when delivered by *Salmonella* in the absence of SopB or SopE (40). The remaining SopE2 activity in the *sopE sopB* double mutant is likely antagonized by SptP (40).

Although the secretion domains of the type III effector molecules have been studied extensively (1, 24, 25, 27, 30–32), very few studies describe the translocation domains. The minimal secretion domain of type III effectors in *Yersinia* and *Salmonella* have been localized to the first ~20 amino acids from the N termini (24, 25, 30, 32). The minimal translocation domain of SptP (amino acids 1 to 159) was identified by functional and crystallographic studies (7, 37). With the ruffling translocation assay, we have determined that additional C-terminal deletions in $SopA_{1–45}$ eliminate its translocation. The translocation of $SopA_{1–45}$ is further supported by the experiment that showed that the $SopA_{1–45}$-CyaA, but not the $SopA_{1–44}$-CyaA, fusion was translocated. $SopA_{1–45}$-CyaA was slightly, but significantly, translocated into Henle-407 compared to $SopA_{1–44}$-CyaA. Since $SopA_{1–45}$, not $SopA_{1–44}$, was able to translocate $SopE_{78–240}$, this further illustrates the sensitivity of the translocation ruffling assay. $SopA_{1–45}$ was translocated at a much lower efficiency than the full-length SopA and approximately 2.5 times more than the negative control. Interestingly, Sop $A_{1–95}$-$SopE_{78–240}$ induced prominent ruffle formation and the $SopA_{1–95}$-CyaA fusion exhibited a high level of cAMP, suggesting that efficient secretion and translocation of SopA requires sequences beyond the minimum $SopA_{1–45}$. We have also found that $SopA_{1–45}$, but not $SopA_{1–44}$, is able to bind to InvB by both yeast two-hybrid and far-Western analyses. This correlation further indicates that $SopA_{1–45}$ is the minimal domain for SPI-1 secretion and translocation. It also further supports the importance of chaperone binding and its role in secretion and/or translocation of SopA.

Previously, Ehrbar et al. showed that $SopA_{1–287}$-M45 secretion is dependent on a functional SPI-1 TTSS with lack of secretion of $SopA_{1–287}$-M45 from the *invC*::*aphT* mutant (6). In this study, we found that SopA-M45 is secreted through both the SPI-1 and the flagellar export apparatuses. We are certain that the SopA secretion in the *invA* mutant is neither due to leakage through the SPI-1 TTSS nor due to the lysis of bacteria. First, we observed SopA secretion in a mutant that contained in-frame deletions in both InvA and InvG, two essential components of the SPI-1 TTSS (data not shown). Second, we found that SopA-M45 secretion was eliminated in the *invB flgGHI* strain but was unaffected in *invB invA* (Fig. 5), indicating that SopA secretion through the SPI-1 TTSS is InvB dependent and is InvB independent when exported through the flagellar transport system. Third, we never detected Hsp60 (3), a *Salmonella* cytosolic protein, in any of the secretion samples tested. Lastly, SopA secretion is completely eliminated in the *invA flgGHI* strain, which is deficient in both SPI-1 TTSS and flagellar secretion, further demonstrating that SopA proteins detected in the *invA* mutant supernatant are due to specific secretion through the flagellar export apparatus.

Several different experimental conditions may have contributed to the discrepancy between our SopA secretion data and those of Ehrbar et al. (6). First, they used an *invC*::*aphT* mutant strain and we used the *invA*::*aphT invA invG* in-frame deletion (data not shown) mutant strains. Second, subtle differences in bacterial culture conditions may need to be examined to see if culture conditions induced/suppressed the expression or the proper function of the flagellar export apparatus. In the absence of a functional flagellar export apparatus, no SopA would be detected in the *invA* mutant strain.

Our data showed that $SopA_{full}$-$SopE_{78–240}$-M45, $SopA_{1–45}$-$SopE_{78–240}$-M45, and $SopA_{1–44}$-$SopE_{78–240}$-M45 were all secreted through the flagellar export apparatus. $SopA_{1–35}$-$SopE_{78–240}$-M45 and $SopA_{1–10}$-$SopE_{78–240}$-M45 are also capable of being secreted through the flagellar export apparatus (data not shown). Further N-terminal truncation resulted in very poor expression of the fusion proteins (data not shown). It is not clear what role the flagellar export of SopA plays in *Salmonella*

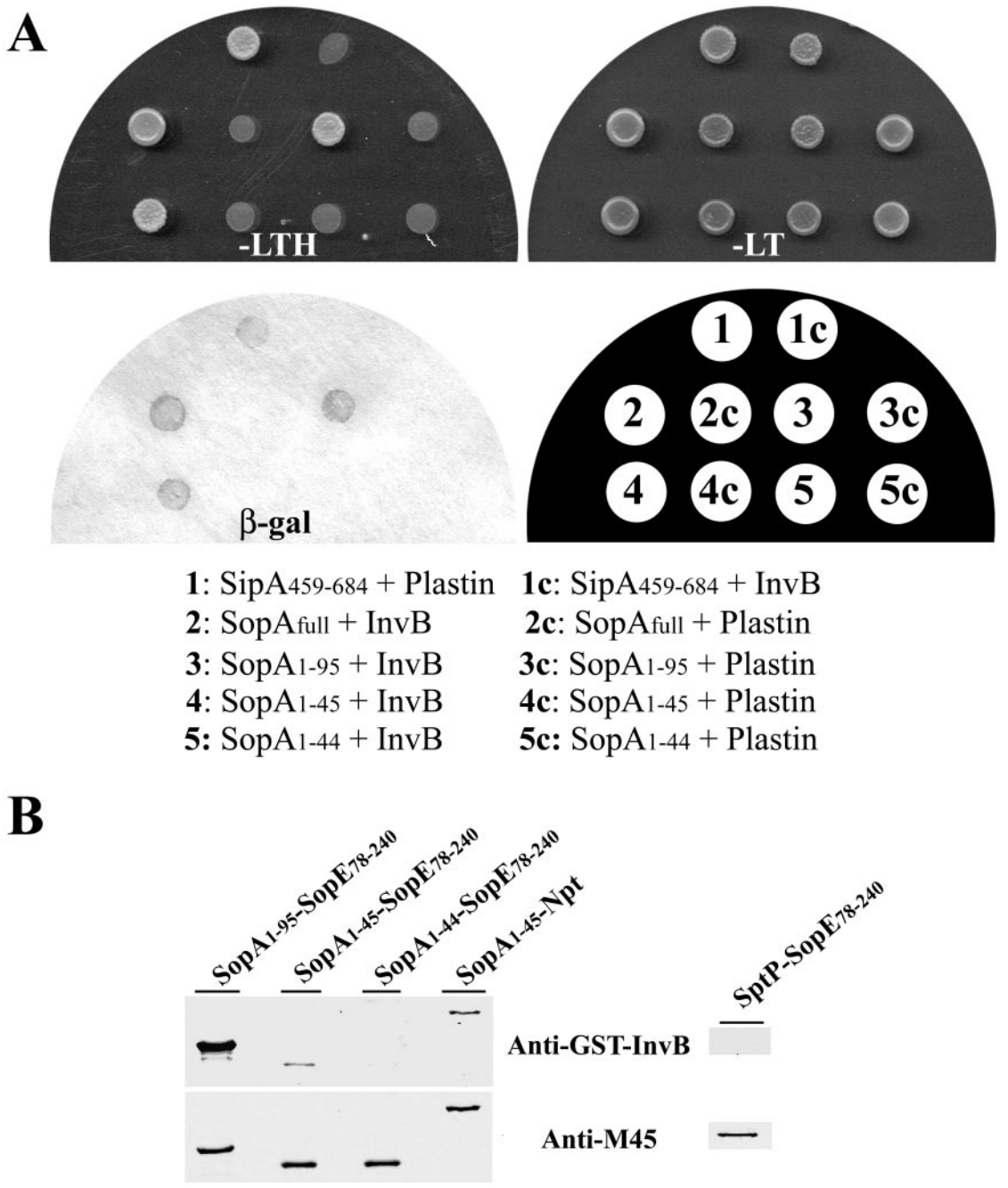

FIG. 7. $SopA_{1–45}$, but not $SopA_{1–44}$, interacts with its chaperone, InvB, as tested by yeast two-hybrid analysis (A) and a protein overlay assay (B). (A) Equivalent amounts of Y153 carrying GAL4-SopA, GAL4-$SopA_{1–95}$-$SopE_{78–240}$, and GAL4-$SopA_{1–45}$-Npt, together with GAL4-InvB, were spotted on the yeast drop-out media with and without histidine. Growth was recorded, and a β-galactosidase lift assay was carried out after 3 days of incubation at 30°C. (B) Equal amounts of whole-cell lysates of *E. coli* DH5α expressing $SopA_{1–95}$-$SopE_{78–240}$-M45, $SopA_{1–45}$-$SopE_{78–240}$-M45, $SopA_{1–44}$-$SopE_{78–240}$-M45, $SopA_{1–45}$-Npt-M45, and $SptP_{1–159}$-$SopE_{78–240}$-M45 were separated by SDS-PAGE and immobilized on nitrocellulose membranes. The membranes were probed with purified GST-InvB or GST alone, followed by anti-GST antibodies (top). Total fusion proteins were probed with anti-M45 monoclonal antibodies (bottom).

pathogenesis. Our data indicate that there is no translocation following the flagellar export of SopA. Further studies are required to investigate whether SopA functions in an extracellular manner in *Salmonella* pathogenesis. In fact, it has been reported that extracellular SipA might activate a PKC-α-dependent signal transduction pathway to induce neutrophil transepithelial migration (20, 35).

In summary, we have determined the minimal secretion and translocation region of SopA to be within the first 45 amino acids. This region binds its chaperone and is sufficient for both

the secretion signal and the translocation signal for the SPI-1 type III apparatus in *Salmonella*. It is clear that the secretion and translocation domains overlap with the chaperone-binding domain, and they may even be the same domain.

ACKNOWLEDGMENTS

We thank Arthur Aronson and Virginia Livingston for critically reviewing the manuscript. We also thank Patrick Hearing for providing monoclonal anti-M45 antibodies.

Research was supported by NIH grant AI49978 to D.Z.

REFERENCES

1. **Anderson, D. M., and O. Schneewind.** 1997. A mRNA signal for the type III secretion of Yop proteins by *Yersinia enterocolitica*. Science **278:**1140–1143.
2. **Bartel, P. L., and S. Fields.** 1995. Analyzing protein-protein interactions using two-hybrid system. Methods Enzymol. **254:**241–263.
3. **Boog, C., E. de Graeff-Meeder, M. Lucassen, R. van der Zee, M. Voorhorst-Ogink, P. van Kooten, H. Geuze, and W. van Eden.** 1992. Two monoclonal antibodies generated against human hsp60 show reactivity with synovial membranes of patients with juvenile chronic arthritis. J. Exp. Med. **175:** 1805–1810.
4. **Bronstein, P. A., E. A. Miao, and S. I. Miller.** 2000. InvB is a type III secretion chaperone specific for SspA. J. Bacteriol. **182:**6638–6644.
5. **Day, J. B., F. Ferracci, and G. V. Plano.** 2003. Translocation of YopE and YopN into eukaryotic cells by *Yersinia pestis yopN*, *tyeA*, *sycN*, *yscB* and *lcrG* deletion mutants measured using a phosphorylatable peptide tag and phosphospecific antibodies. Mol. Microbiol. **47:**807–823.
6. **Ehrbar, K., S. Hapfelmeier, B. Stecher, and W. D. Hardt.** 2004. InvB is required for type III-dependent secretion of SopA in *Salmonella enterica* serovar Typhimurium. J. Bacteriol. **186:**1215–1219.
7. **Fu, Y., and J. E. Galán.** 1998. Identification of a specific chaperone for SptP, a substrate of the centisome 63 type III secretion system of *Salmonella typhimurium*. J. Bacteriol. **180:**3393–3399.
8. **Fu, Y., and J. E. Galán.** 1998. The *Salmonella typhimurium* tyrosine phosphatase SptP is translocated into host cells and disrupts the actin cytoskeleton. Mol. Microbiol. **27:**359–368.
9. **Galán, J. E., and R. D. Curtiss.** 1989. Cloning and molecular characterization of genes whose products allow *Salmonella typhimurium* to penetrate tissue culture cells. Proc. Natl. Acad. Sci. USA **86:**6383–6387.
10. **Galán, J. E., C. Ginocchio, and P. Costeas.** 1992. Molecular and functional characterization of the *Salmonella* invasion gene *invA*: homology of InvA to members of a new protein family. J. Bacteriol. **174:**4338–4349.
11. **Goss, J. W., J. A. Sorg, K. S. Ramamurthi, H. Ton-That, and O. Schneewind.** 2004. The secretion signal of YopN, a regulatory protein of the *Yersinia enterocolitica* type III secretion pathway. J. Bacteriol. **186:**6320–6324.
12. **Hardt, W.-D., L.-M. Chen, K. E. Schuebel, X. R. Bustelo, and J. E. Galán.** 1998. *Salmonella typhimurium* encodes an activator of Rho GTPases that induces membrane ruffling and nuclear responses in host cells. Cell **93:**815–826.
13. **Hardt, W. D., H. Urlaub, and J. E. Galán.** 1998. A substrate of the centisome 63 type III protein secretion system of *Salmonella typhimurium* is encoded by a cryptic bacteriophage. Proc. Natl. Acad. Sci. USA **95:**2574–2579.
14. **Hoiseth, S. K., and B. A. Stocker.** 1981. Aromatic-dependent *Salmonella typhimurium* are non-virulent and effective as live vaccines. Nature **291:**238–239.
15. **Kaniga, K., J. C. Bossio, and J. E. Galán.** 1994. The *Salmonella typhimurium* invasion genes *invF* and *invG* encode homologues of the AraC and PulD family of proteins. Mol. Microbiol. **13:**555–568.
16. **Kaniga, K., I. Delor, and G. R. Cornelis.** 1991. A wide-host-range suicide vector for improving reverse genetics in Gram-negative bacteria: inactivation of the *blaA* gene of *Yersinia enterocolitica*. Gene **109:**137–141.
17. **Kaniga, K., D. Trollinger, and J. E. Galán.** 1995. Identification of two targets of the type III protein secretion system encoded by the *inv* and *spa* loci of *Salmonella typhimurium* that have homology to the *Shigella* IpaD and IpaA proteins. J. Bacteriol. **177:**7078–7085.
18. **Karavolos, M. H., M. Wilson, J. Henderson, J. J. Lee, and C. M. Khan.** 2005. Type III secretion of the *Salmonella* effector protein SopE is mediated via an N-terminal amino acid signal and not an mRNA sequence. J. Bacteriol. **187:**1559–1567.
19. **Kubori, T., Y. Matsushima, D. Nakamura, J. Uralil, M. Lara-Tejero, A. Sukhan, J. E. Galán, and S. I. Aizawa.** 1998. Supramolecular structure of the *Salmonella typhimurium* type III protein secretion system. Science **280:**602–605.
20. **Lee, C. A., M. Silva, A. M. Siber, A. J. Kelly, E. Galyov, and B. A. McCormick.** 2000. A secreted *Salmonella* protein induces a proinflammatory response in epithelial cells, which promotes neutrophil migration. Proc. Natl. Acad. Sci. USA **97:**12283–12288.
21. **Lee, S. H., and J. E. Galán.** 2003. InvB is a type III secretion-associated chaperone for the *Salmonella enterica* effector protein SopE. J. Bacteriol. **185:**7279–7284.
22. **Lee, V. T., D. M. Anderson, and O. Schneewind.** 1998. Targeting of *Yersinia* Yop proteins into the cytosol of HeLa cells: one-step translocation of YopE across bacterial and eukaryotic membranes is dependent on SycE chaperone. Mol. Microbiol. **28:**593–601.
23. **Lloyd, S. A., M. Norman, R. Rosqvist, and H. Wolf-Watz.** 2001. *Yersinia* YopE is targeted for type III secretion by N-terminal, not mRNA, signals. Mol. Microbiol. **39:**520–531.
24. **Miao, E. A., and S. I. Miller.** 2000. A conserved amino acid sequence directing intracellular type III secretion by *Salmonella typhimurium*. Proc. Natl. Acad. Sci. USA **97:**7539–7544.
25. **Miao, E. A., C. A. Scherer, R. M. Tsolis, R. A. Kingsley, L. G. Adams, A. J. Baumler, and S. I. Miller.** 1999. *Salmonella typhimurium* leucine-rich repeat proteins are targeted to the SPI1 and SPI2 type III secretion systems. Mol. Microbiol. **34:**850–864.
26. **Miller, V. L., and J. J. Mekalanos.** 1988. A novel suicide vector and its use in construction of insertion mutations: osmoregulation of outer membrane proteins and virulence determinants in *Vibrio cholerae* requires *toxR*. J. Bacteriol. **170:**2575–2583.
27. **Mudgett, M. B., O. Chesnokova, D. Dahlbeck, E. T. Clark, O. Rossier, U. Bonas, and B. J. Staskawicz.** 2000. Molecular signals required for type III secretion and translocation of the *Xanthomonas campestris* AvrBs2 protein to pepper plants. Proc. Natl. Acad. Sci. USA **97:**13324–13329.
28. **Page, A. L., and C. Parsot.** 2002. Chaperones of the type III secretion pathway: jacks of all trades. Mol. Microbiol. **46:**1–11.
29. **Pickard, D., J. Li, M. Roberts, D. Maskell, D. Hone, M. Levine, G. Dougan, and S. Chatfield.** 1994. Characterization of defined *ompR* mutants of *Salmonella typhi*: *ompR* is involved in the regulation of Vi polysaccharide expression. Infect. Immun. **62:**3984–3993.
30. **Ramamurthi, K. S., and O. Schneewind.** 2003. Substrate recognition by the *Yersinia* type III protein secretion machinery. Mol. Microbiol. **50:**1095–1102.
31. **Ramamurthi, K. S., and O. Schneewind.** 2002. Type III protein secretion in *Yersinia species*. Annu. Rev. Cell Dev. Biol. **18:**107–133.
32. **Ramamurthi, K. S., and O. Schneewind.** 2003. *Yersinia yopQ* mRNA encodes a bipartite type III secretion signal in the first 15 codons. Mol. Microbiol. **50:**1189–1198.
33. **Rosqvist, R., A. Forsberg, and W. H. Wolf.** 1991. Intracellular targeting of the *Yersinia* YopE cytotoxin in mammalian cells induces actin microfilament disruption. Infect. Immun. **59:**4562–4569.
34. **Sampson, J. S., S. P. O'Connor, A. R. Stinson, J. A. Tharpe, and H. Russell.** 1994. Cloning and nucleotide sequence analysis of *psaA*, the *Streptococcus pneumoniae* gene encoding a 37-kilodalton protein homologous to previously reported *Streptococcus* sp. adhesins. Infect. Immun. **62:**319–324.
35. **Silva, M., C. Song, W. J. Nadeau, J. B. Matthews, and B. A. McCormick.** 2004. *Salmonella typhimurium* SipA-induced neutrophil transepithelial migration: involvement of a PKC-alpha-dependent signal transduction pathway. Am. J. Physiol. Gastrointest. Liver Physiol. **286:**G1024–G1031.
36. **Sory, M. P., and G. R. Cornelis.** 1994. Translocation of a hybrid YopE-adenylate cyclase from *Yersinia enterocolitica* into HeLa cells. Mol. Microbiol. **14:**583–594.
37. **Stebbins, C. E., and J. E. Galán.** 2001. Maintenance of an unfolded polypeptide by a cognate chaperone in bacterial type III secretion. Nature **414:**77–81.
38. **Wood, M. W., M. A. Jones, P. R. Watson, A. M. Siber, B. A. McCormick, S. Hedges, R. Rosqvist, T. S. Wallis, and E. E. Galyov.** 2000. The secreted effector protein of *Salmonella dublin*, SopA, is translocated into eukaryotic cells and influences the induction of enteritis. Cell. Microbiol. **2:**293–303.
39. **Zhang, S., R. L. Santos, R. M. Tsolis, S. Stender, W. D. Hardt, A. J. Baumler, and L. G. Adams.** 2002. The *Salmonella enterica* serotype Typhimurium effector proteins SipA, SopA, SopB, SopD, and SopE2 act in concert to induce diarrhea in calves. Infect. Immun. **70:**3843–3855.
40. **Zhou, D., L. M. Chen, L. Hernandez, S. B. Shears, and J. E. Galán.** 2001. A *Salmonella* inositol polyphosphatase acts in conjunction with other bacterial effectors to promote host cell actin cytoskeleton rearrangements and bacterial internalization. Mol. Microbiol. **39:**248–259.
41. **Zhou, D., M. S. Mooseker, and J. E. Galán.** 1999. An invasion-associated *Salmonella* protein modulates the actin-bundling activity of plastin. Proc. Natl. Acad. Sci. USA **96:**10176–10181.
42. **Zhou, D., M. S. Mooseker, and J. E. Galán.** 1999. Role of the *S. typhimurium* actin-binding protein SipA in bacterial internalization. Science **283:**2092–2095.